Estimation of 2D Position and Flatness Errors for a Planar XY Stage Based on Measured Guideway Profiles

Jooho Hwang[1,#], Chun-Hong Park[1] and Seung-Woo Kim[2]

1Intelligent Machine Research Center, Korea Institute of Machinery and Materials, Daejeon, South Korea
2Department of Mechanical Engineering, Korea Advanced Institute of Science and Technology, Daejeon, South Korea
#Corresponding Author / E-MAIL: jooho@kimm.re.kr; TEL: +82-42-868-7119; FAX: +82-42-868-7180

KEYWORDS: Planar XY stage, Profile measurement, Motion error, 2D position error, Flatness

Aerostatic planar XY stages are frequently used as the main frames of precision positioning systems. The machining and assembly process of the rails and bed of the stage is one of first processes performed when the system is built. When the system is complete, the 2D position, motion, and stage flatness errors are measured in tests. If the stage errors exceed the application requirements, the stage must be remachined and the assembly process must be repeated. This is difficult and time-consuming work. In this paper, a method for estimating the errors of a planar XY stage is proposed that can be applied when the rails and bed of the stage are evaluated. Profile measurements, estimates of the motion error, and 2D position estimation models were considered. A comparison of experimental results and our estimates indicated that the estimated errors were within 1 μm of their true values. Thus, the proposed estimation method for 2D position and flatness errors of an aerostatic planar XY stage is expected to be a useful tool during the assembly process of guideways.

Manuscript received: May 1, 2006 / Accepted: December 22, 2006

1. Introduction

A planar XY stage is frequently used as a precision positioning system for equipment that produces semiconductors or flat panel displays. Therefore, higher velocities and better accuracies are required to attain higher productivity and performance measures. A planar XY stage, for which an H-shaped frame is usually used as the base stage, is driven by two actuators, such as linear motors, with two position feedback sensors, such as linear scales or interferometers on the scanning motion axis. The stage is frequently used as the main frame of the equipment. Therefore, the machining and assembly process of the rails and bed of the stage is one of first processes performed when the equipment is built. The 2D position, motion, and stage flatness errors are measured when the system is tested after it is complete. If the stage errors do not meet the required specifications, the stage must be remachined and assembly process must be repeated. This is difficult and time-consuming work, especially when the assembly and disassembly process must be repeated for a large stage.

In this paper, a method to estimate the errors of a planar XY stage was proposed that can be applied when the rails and bed of the stage are evaluated. The estimation procedure requires three steps. First, the profiles of a pair of guideways are measured using a sequential two-point method and an extended reversal method.[1] Then the motion errors of the X- and Y-axes are estimated using the static equilibrium of an aerostatic bearing obtained from the measured profiles.[2] Finally, the 2D position and flatness errors are estimated using a homogeneous transformation matrix model from the estimated motion errors of the X- and Y-axes.[3] The estimated results are compared with the 2D position and flatness errors obtained from the motion errors measured by a laser interferometer.

2. Configuration of the planar XY stage

As shown in Fig. 1, the moving table of a planar XY stage translates along the X-axis on the base stage, which has an H-type structure and is driven by two simultaneously controlled linear motors (LM310-4, Trilogy) along the Y-axis. The stroke of each axis is 300 mm, which can be measured using a precise optical linear scale (LIP481, HeidenHain). A PC-based motion control board with a PID filter (PMAC2, Delta Tau) is used to control the position of the stage. The X- and Y-axes move on a granite bed, which is used as a vertical guide for the vacuum preloaded aerostatic bearings of the two stages to avoid deflections of the table and base stage and to reduce the

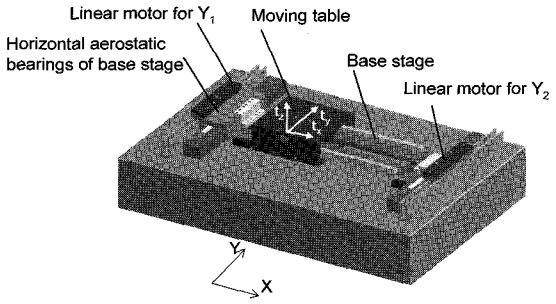

Fig. 1 Schematic diagram of a planar XY stage

moment forces in high acceleration motions. A double pad aerostatic bearing is used to constrain the horizontal motion. As shown in Fig. 1, the base stage is constrained against the horizontal motion only at the aerostatic bearing on the Y_1 axis.

3. Guideway profile measurements

Guideways are important elements of a planar XY stage. They usually consist of a pair of surfaces that provide a constraint in one direction, along with bearings. Noncontact bearings, such as hydrostatic or aerostatic bearings, are usually adopted for ultraprecision guideways, in which the profiles of the rails affect the straightness of the table and the clearance of the bearings affects the stiffness of the guideways. The clearance is varied along the moving table according to the relative distance between the pair of rails. This is often referred to as the parallelism of the two rails. Several methods are used to obtain a measure of the straightness of each rail, such as the reversal,[4-6] sequential two-point,[7-12] and multi-probe[13-17] methods. These methods generally acquire deviation profiles by eliminating a linear fitted inclined curve; however, they seldom provide information about the relative distance between the pair of rails.[18] This section describes a method for simultaneously measuring the parallelism and straightness of a pair of rails. The profiles of a pair of rails were measured using three displacement probes and a probe stage.

3.1 Parallelism measurements

A schematic diagram of the three-probe parallelism and straightness measurement system for typical guideways is shown in Fig. 2. The probe stage, which carries the three probes, moves along the pair of rails. Two of the three probes, P_1 and P_2, are used for the parallelism measurements. The profiles of Rail 1 and Rail 2 are described by $f(x)$ and $g(x)$, respectively. The corresponding measurement data, $m_1(x)$ and $m_2(x)$, are

$$\begin{aligned} m_1(x_i) &= f(x_i) - e_1(x_i) \\ m_2(x_i) &= -\big(g(x_i) - e_2(x_i)\big) \\ e_1(x_i) &= \delta_y(x_i) + t_{x1}\varepsilon_z(x_i) - t_{z1}\varepsilon_x(x_i) + \theta_y \cdot x_i \\ e_2(x_i) &= \delta_y(x_i) + t_{x2}\varepsilon_z(x_i) - t_{z2}\varepsilon_x(x_i) + \theta_y \cdot x_i \end{aligned}, \quad (1)$$

where $e_1(x_i)$ and $e_2(x_i)$ are the measuring errors due to the probe stage; $\delta_y(x_i)$, $\varepsilon_z(x_i)$, $\varepsilon_x(x_i)$, and θ_y are the y-direction straightness, yaw error, roll error, and alignment error of the probe stage along the x-axis, respectively; and $t_{x1}(x_i)$, $t_{x2}(x_i)$, $t_{z1}(x_i)$, and $t_{z2}(x_i)$ are the x- and z-direction constant offset values of P_1 and P_2. The negative sign of $m_2(x_i)$ in Eq. (1) indicates the negative sensitivity of P_2 in the $+y$ direction. Summing the two measured sets of data in Eq. (1) and setting $t_{x1} = t_{x2}$ and $t_{z1} = t_{z2}$ gives

$$\begin{aligned} p(x_i) &= m_1(x_i) + m_2(x_i) \\ &= f(x_i) - g(x_i) - e_1(x_i) + e_2(x_i), \\ &= f(x_i) - g(x_i) \end{aligned} \quad (2)$$

Equation (2) describes the deviation of the two profiles along the X-axis, or the parallelism of the pair of rails. This procedure is known as the reversal method, and its cancellation effect has been used in many other studies.[4-6]

The slope between the two rails can be defined using a linear least squares fit method, expressed as

$$\alpha = \frac{n\sum_{i=1}^{n} x_i p(x_i) - \sum_{i=1}^{n} x_i \sum_{i=1}^{n} p(x_i)}{n\sum_{i=1}^{n} x_i^2 - \left(\sum_{i=1}^{n} x_i\right)^2}, \quad (3)$$

From Eqs. (2) and (3), the principle of allotment, which is applicable when acquiring slopes, is

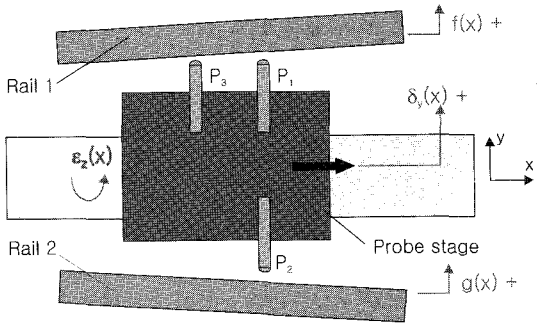

Fig. 2 Setup for measuring parallelism and straightness

$$\begin{aligned} \alpha &= \frac{n\sum_{i=1}^{n} x_i f(x_i) - n\sum_{i=1}^{n} x_i g(x_i) - \sum_{i=1}^{n} x_i \sum_{i=1}^{n} f(x_i) + \sum_{i=1}^{n} x_i \sum_{i=1}^{n} g(x_i)}{n\sum_{i=1}^{n} x_i^2 - \left(\sum_{i=1}^{n} x_i\right)^2}, \quad (4) \\ &= a_1 - a_2 \end{aligned}$$

where a_1 and a_2 are the slopes of $f(x)$ and $g(x)$, respectively. Consequently, the difference between the slopes of the two rails can be calculated.

3.2 Simultaneous parallelism and straightness measurements

The straightness of each rail is also an important factor for guideways. To measure the straightness of each rail for horizontal guideways, a third displacement probe was attached to the system, as shown in Fig. 1. The measured data for each probe can be expressed as

$$\begin{aligned} m_1(x_i) &= f_d(x_i) - e_1(x_i) \\ m_3(x_i) &= f_d(x_{i-1}) - e_3(x_i) \\ e_3(x_i) &= \delta_y(x_i) + t_{x3}\varepsilon_z(x_i) - t_{z3}\varepsilon_x(x_i) + \theta_y \cdot x_i \end{aligned}, \quad (5)$$

where $t_{x3}(x_i)$ and $t_{z3}(x_i)$ are the x- and z-direction constant offset values of P_3, and $f_d(x)$ is similar to $f(x)$ except that the initial measured values of $m_1(x)$ and $m_3(x)$ were set to 0 and the profile was calculated from incremental values. When $t_{z1} = t_{z3}$ and the measuring step is the same as the distance between the probes, $l = t_{x1} - t_{x3}$, the profiles of Rails 1 and 2 can be expressed from Eq. (2) and

$$\begin{aligned} f(x_i) &\approx f_d(x_i) = f_d(x_{i-1}) + m_1(x_i) - m_3(x_i) + l\varepsilon_z(x_i) \\ g_d(x_i) &\approx f_d(x_i) - P(x_i) \end{aligned}, \quad (6)$$

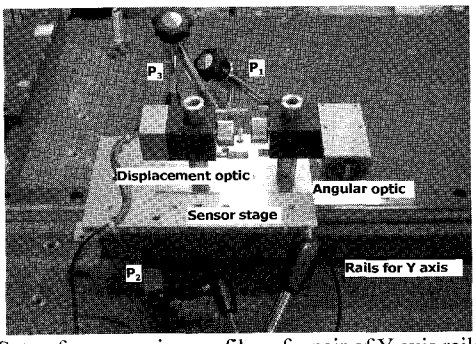

Fig. 3 Setup for measuring profiles of a pair of Y-axis rails

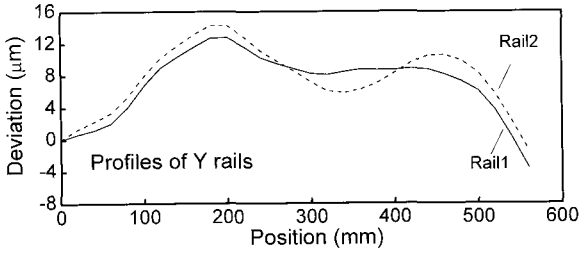

Fig. 4 Profiles of the Y-axis rails

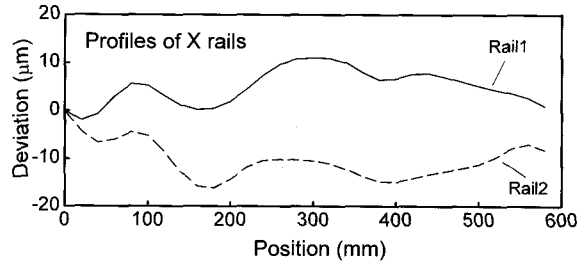

Fig. 5 Profiles of X-axis rails

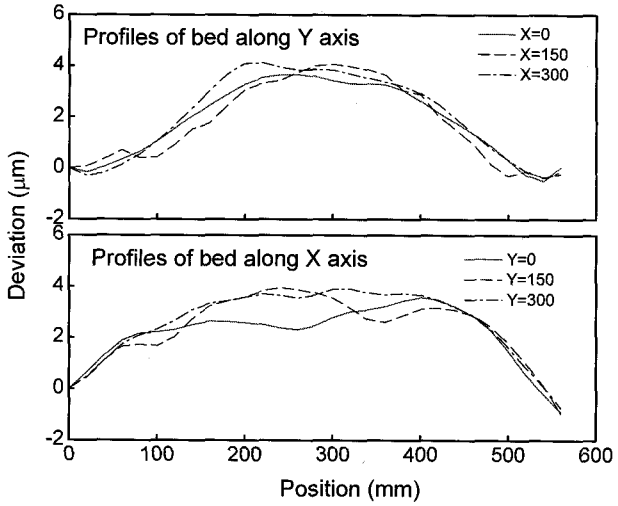

Fig. 6 Measured profile of the bed along the X- and Y-axes

Equation (6) uses a sequential two-point method to eliminate the stage error, as described in previous studies.[7-12] The angular error of the probe stage is required in order to use Eq. (6). This must be measured using an autocollimator or a laser interferometer.[19]

To measure the profiles of the guideways for the X- and Y-axes, three inductive probes (Mahr, 1320/1) and an angular interferometer were fixed in the manual stage, which had a displacement interferometer to detect its position, as shown in Fig. 3.

The measured profiles of each guideway are shown in Figs. 4–6. The vertical guideways of the X- and Y-axes are the surface of the bed. The surface profiles were interpolated from the measured data shown in Fig. 6 along six different positions at which the center of the stage will be located.

4. Estimation of the motion error

4.1 Static equilibrium model of the stage

The static equilibrium modeling, which considers the change in the reaction force and displacement for a single porous pad of the aerostatic stage, is shown in Fig. 7, where W is the external load of the table including its weight, m is the number of pads in the table, X_{ci} is the distance from the center of the table to the center of the pads, L is the length of the rails, and $F_i(x)$ and $Z_i(x)$ are the i^{th} reaction force

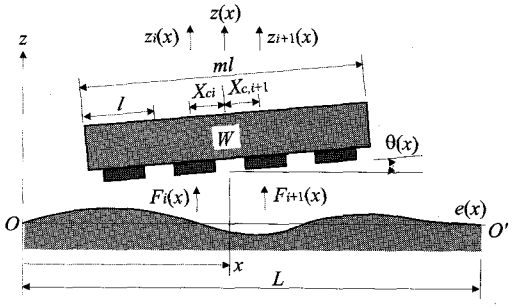

Fig. 7 Equilibrium state of a porous aerostatic stage

and corresponding displacement of the center of the pads. The position of the center of the table is x, and $\theta(x)$ is the slope of the table.

If the relationship between the rail profiles and each pad of the table is considered, the pad of the table is moved to a new equilibrium state due to the changed aerostatic reaction force ($f_{ei}(x)$) and new stage displacement ($z_i(x)$); the reaction force is $F_i(x)$.

Assuming that the stiffness of the aerostatic pads is constant within the small displacement of the stage, the relationship between $f_{ei}(x)$ and $z_i(x)$ is

$$f_i(x) = f_{ei}(x) - K_0 z_i(x), \tag{7}$$

Considering Eq. (7), the moment equilibrium from the reaction force of the pads is

$$\sum_{i=1}^{m} \{f_{ei}(x) - K_0 z_i(x)\} = 0, \tag{8}$$

$$\sum_{i=1}^{m} f_{ei}(x)\left(X_{ci} - R_i(x) + \frac{ml}{2}\right) = \sum_{i=1}^{m} K_0 z_i(x)\left(X_{ci} + \frac{ml}{2}\right), \quad x = \frac{ml}{2}, \cdots, L - \frac{ml}{2} \tag{9}$$

The Fourier transformed profiles of the rails ($e(x)$) is then

$$e(x) = a_0 + \sum_{k=1}^{n}\left(a_k \cos\frac{2k\pi}{L}x + b_k \sin\frac{2k\pi}{L}x\right), \tag{10}$$

4.2 Computation of the motion error

The aerostatic bearing pads of the stage are the same shape and have a multi-supported configuration in the same plane, as shown in Fig. 7. Therefore, the error motion of the moving table of the stage can be calculated from the geometric relationship of each pad and the calculated characteristic of one pad. This can be calculated quickly during the assembly process of the stage.

When a porous pad is moving along the rails and the center of the pad has the same coordination as the rails, the profiles of the rails in Eq. (5) and the change of the reaction force of a porous pad ($f_e(x)$) can be explained using the spatial frequency (ω). The spatial frequency is defined as $\omega = 2\pi/\lambda$, where the wavelength for one sinusoidal profile of the rails is defined as λ. When the wavelength is the same as the length of the pad (l), the spatial frequency becomes $\omega_l = 2\pi/l$. The change of the reaction force ($f_e(x)$) has the same spatial frequency as the rails if the profile of the rail $e(x)$ has only a single spatial frequency ω. From this relationship, the motion transfer function may be defined as

$$K(\omega) = \frac{f_e(\omega)}{e(\omega)}, \tag{11}$$

The linear motion error and angular motion error can be represented by

$$z(x) = \frac{1}{K_0 m}\sum_{i=1}^{m} f_e(x + X_{ci}), \quad \theta(x) = \frac{12}{K_0 m(m^2-1)l^2}\sum_{i=1}^{m}\{f_e(x+X_{ci})(X_{ci} - R_i(x+X_{ci}))\} \tag{12}$$

where $f_e(x)$ and $R(x)$ can be represented by Eqs. (8) and (9),[2] yielding

$$f_e(x) = \sum_{k=1}^{n} K\left(\frac{2k\pi}{L}\right)\left(a_k \cos\frac{2k\pi}{L}x + b_k \sin\frac{2k\pi}{L}x\right), \tag{13}$$

$$R(x) = l\sum_{k=1}^{n} G\left(\frac{2k\pi}{L}\right)\left(a_k \cos\frac{2k\pi}{L}x + b_k \sin\frac{2k\pi}{L}x\right), \tag{14}$$

The motion errors of the stage can be acquired by sequential repetitive calculations along the moving directions.

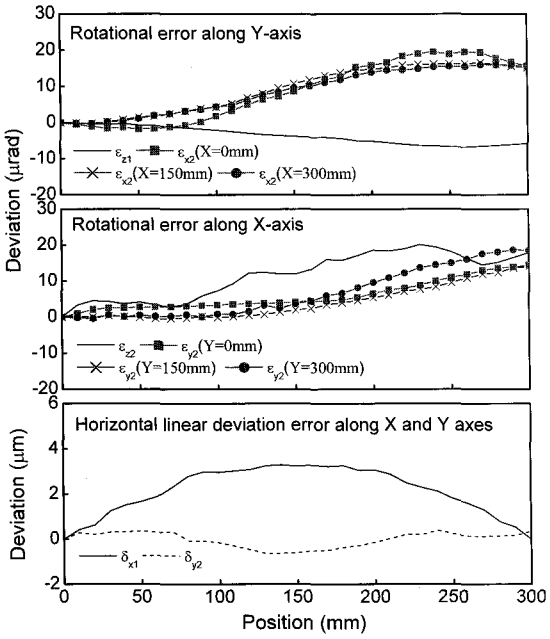

(a) measured motion errors

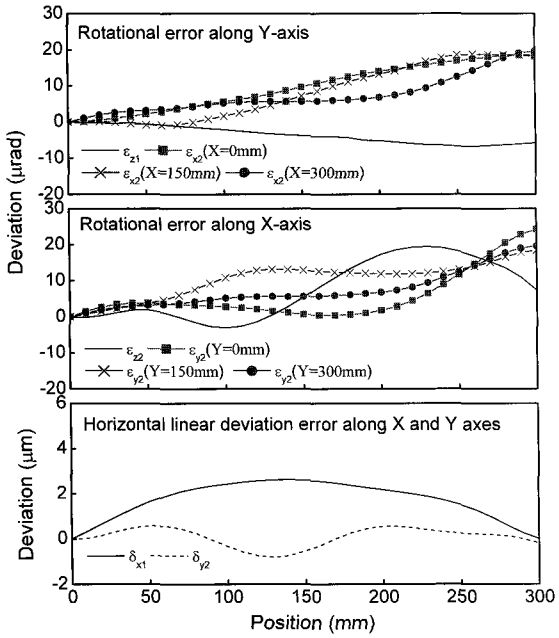

(b) estimated motion errors

Fig. 8 Comparison between measured and estimated motion errors of the planar XY stage

5. Estimation of the 2D position and flatness errors

The 2D position error estimation model of the planar XY stage was introduced about the same stage. It is represented by[3]

$$\begin{bmatrix}\delta P_x(i,j)\\ \delta P_y(i,j)\end{bmatrix}=\begin{bmatrix}-t_y\left(\varepsilon_{z1}(j)+\varepsilon_{z2}(i)\right)+t_z\varepsilon_{y2}(i,j)+\delta x_1(j)+\delta x_2(i)\\ t_x\left(\varepsilon_{z1}(j)+\varepsilon_{z2}(i)\right)-t_z\varepsilon_{x2}(i,j)+a_2(i)\varepsilon_{z1}(j)+a_2(i)\theta_{12}+\delta y_1(j)+\delta y_2(i)\end{bmatrix}, \quad (15)$$

In Eq. (15), each error motion contains an i or j index, or both. These are intermittent steps of the estimation and measurement process of the 2D error in the X- and Y-directions, respectively. The motion errors of the stage measured by interferometer, shown in Figs. 4–6, and estimated by Eq. (13) are compared in Fig. 8. The yaw motion of base stage (ε_{z1}) is affected by the controlled position of the y1 and y2

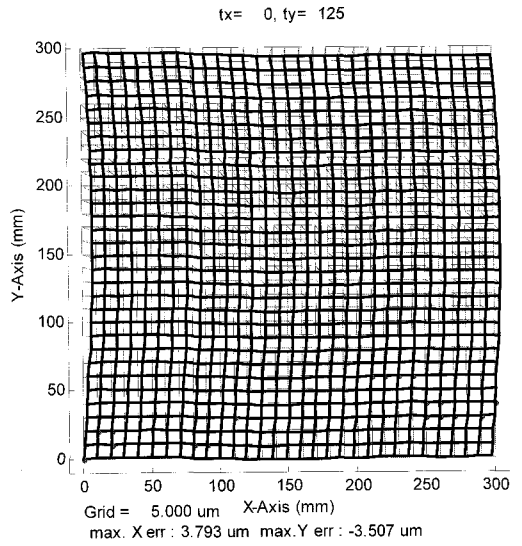

(a) based on the measured motion errors

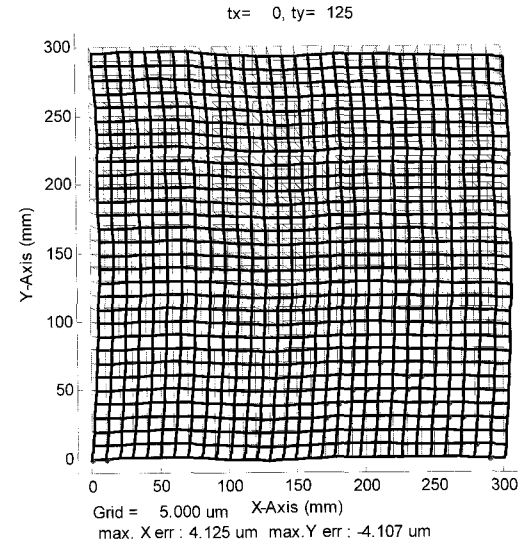

(b) based on the estimated motion errors

Fig. 9 Comparison of 2D position errors at the center of the planar XY stage

axes. Therefore, the measured data of ε_{z1} were used to estimate the 2D position in both cases. As shown in Fig. 8, most of the motion errors were similar, but the yaw motion of the moving table along the X axis had a slightly different shape.

The 2D position error of the stage was estimated from the sum of the motion errors every 10 mm over the 300 × 300-mm translational area. The 2D position errors are compared in Fig. 9 for t_x = 0 mm, t_y = 125 mm, t_z = 60 mm, and θ_{12} = 0. Interpolation was used to estimate the pitch errors $\varepsilon_{x2}(i,j)$ and $\varepsilon_{y2}(i,j)$, which had similar shapes at the three different measured positions because the position difference of 150 mm was less than the span of the aerostatic bearings of the moving table (270 mm). The maximum difference of the measured and estimated position errors was about 0.5 μm.

The straightness of the flatness can simply be calculated from the summation of each interpolated straightness data point, which can be measured directly or estimated from the measured profile data. The comparison of the flatness data is shown in Fig. 10. The maximum difference of the flatness error between the measured and estimated values was about 0.6 μm. These results indicate that the proposed estimation method for 2D position and flatness errors on an aerostatic planar XY stage will be useful in the assembly process of guideways.

6. Conclusions

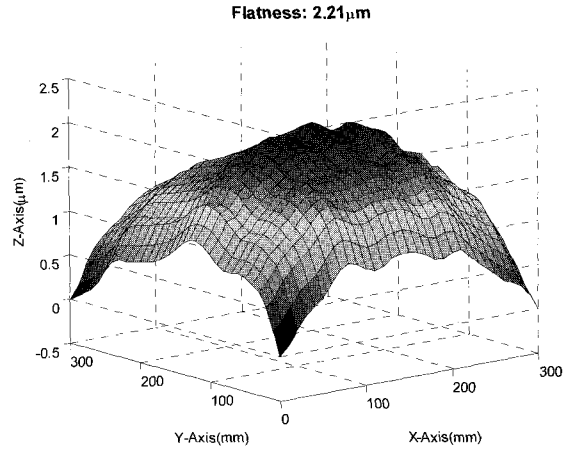

(a) based on the measured straightness

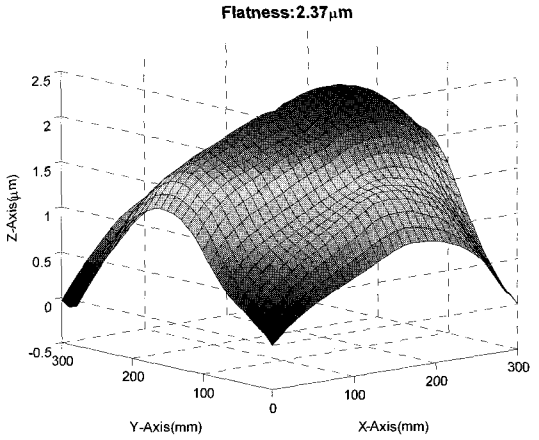

(b) based on the estimated straightness

Fig. 10 Comparison between the measured and estimated flatness

In this paper, an estimation method was proposed for 2D position and flatness errors on an aerostatic planar XY stage. The error was estimated from the estimated motion error obtained using profile measurements of the guideways. Three steps were required to estimate the planar XY stage errors. First, the profiles of a pair of guideways were measured using a sequential two-point method and an extended reversal method. Then the motion errors of the X- and Y-axes were estimated using the static equilibrium of the aerostatic bearing from the measured profiles. Finally, the 2D position and flatness errors were estimated using a homogeneous transformation matrix model from the estimated motion errors of the X- and Y-axes. A comparison of experimental and estimated results demonstrated that the estimates were within 1 μm. Thus, the proposed estimation method for 2D position and flatness errors on an aerostatic planar XY stage can be successfully applied to the assembly process of guideways.

ACKNOWLEDGMENT

The author gratefully acknowledges the support of the Ministry of Commerce, Industry, and Energy (MOCIE) under the "Core Technology Development for Multi-functional Ultra-Precision Machines to Generate Micro Features on Large Surfaces" project.

REFERENCES

1. Hwang, J., Park C. H., Gao, W. and Kim, S. W., "A three-probe method for measuring parallelism and straightness of a pair of rails for ultra precision machine tools," Proceedings of the ASPE 2005 Annual Meeting, pp. 315–318, 2005.
2. Park, C. H. and Lee, H., "Motion error analysis of the porous air bearing stage using the transfer function," Journal of the KSPE, Vol. 21, No. 7, pp. 185–194, 2004.
3. Hwang, J., Park, C. H., Lee, C. H. and Kim, S. W., "Estimation and correction method for the two-dimensional position errors of a planar XY stage based on motion error measurements," International Journal of Machine Tools and Manufacture, Vol. 46, pp. 801–810, 2006.
4. Donaldson, R. R., "A simple method for separating spindle error from test ball roundness error," Annual CIRP, Vol. 21, pp. 125–126, 1972.
5. Estler, W. T., "Calibration and use of optical straightedges in the metrology of precision machines," Optical Engineering, Vol. 24, pp. 372–379, 1985.
6. Evans, C. J., Hocken, R. J. and Estler, W. T., "Self-calibration: Reversal, redundancy, error separation and absolute testing," Annual CIRP, Vol. 45, pp. 617–624, 1996.
7. Tanaka, H., Tazawa, K., Sato, H., O-hori, M. and Sekiguchi, H., "Application of a new straightness measurement method to large machine tools," Annual CIRP, Vol. 30, pp. 455–459, 1981.
8. Tazawa, K., Sato, H. and O-hori, M., "A new method for the measurement of the straightness of machine tools and machined work," ASME Journal of Mechanical Design, Vol. 104, pp. 587–592, 1982.
9. Kiyono, S. and Gao, W., "Profile measurement of machined surface with a new differential method," Precision Engineering, Vol. 16, pp. 212–218, 1994.
10. Gao, W. and Kiyono, S., "High accuracy profile measurement of a machined surface by the combined method," Measurement, Vol. 19, pp. 55–64, 1996.
11. Makosch, G. and Drollinger, B., "Surface profile measurement with a scanning differential AC interferometer," Applied Optics, Vol. 23–24, pp. 4544–4553, 1984.
12. Tanaka, H. and Sato, H., "Extensive analysis and development of straightness measurement by sequential two-point method," Transactions of the ASME, Vol. 108, pp. 176–182, 1986.
13. Fung, E. H. K. and Yang, S. M., "An approach to on-machine motion error measurement of a linear slide," Measurement, Vol. 29, pp. 51–62, 2001.
14. Kounosu, K. and Kishi, T., "Measurement of surface profile using smoothed serial three point method," Journal of JSPE, Vol. 61, pp. 641–645, 1995.
15. Gao, W. and Kiyono, S., "On-machine measurement of machined surface using the combined three-point method," JSME International Journal, Vol. 40, pp. 253–259, 1997.
16. Gao, W., Yokoyama, J., Kojima, H. and Kiyono, S., "Precision measurement of cylinder straightness using a scanning multi-probe system," Precision Engineering, Vol. 26, pp. 279–288, 2002.
17. Yamaguchi, K., "Measurement of straight motion accuracy using the improved sequential three-point method," Journal of the JSPE, Vol. 59, pp. 773–778, 1993.
18. Furukawa, M., Gao, W., Shimizu, H., Kiyono, S., Yasutake, M. and Takahashi, K., "Three-dimensional slit width measurement for long precision slot die," Key Engineering Materials, Vol. 295–296, pp. 343–348, 2005.

19. Gao, W., Yokoyama, J., Kiyono, S. and Hitomi, N., "A scanning multi-probe straightness measurement system for alignment of linear collider accelerator," Key Engineering Materials, Vol. 295–296, pp. 253–258, 2005.